

Three-dimensional imaging of human skin and mucosa by two-photon laser scanning microscopy

Background: Various structural components of human skin biopsy specimens are difficult to visualize using conventional histologic approaches.

Methods: We used two-photon microscopy and advanced imaging software to render three-dimensional (3D) images of *in situ* nerves, blood vessels, and hair follicles labeled with various fluorescent markers. Archived frozen human skin biopsy specimens were cryosectioned up to 150 µm in thickness and fluorescently stained with rhodamine- or fluorescein-labeled antibodies or lectins. Optical sections were collected by two-photon microscopy and the resulting data sets were analyzed in three dimensions using Voxx software.

Results: Reconstructed image volumes demonstrated the complex 3D morphology of nerves, blood vessels and adnexal structures in normal mucocutaneous tissue.

Conclusion: Two-photon microscopy and Voxx rendering software allow for detailed 3D visualization of structures within human mucocutaneous biopsy specimens, as they appear *in situ*, and facilitate objective interpretation of variations in their morphology. These techniques may be used to investigate disorders involving cutaneous structures that are difficult to visualize by means of traditional microscopy.

Malone JC, Hood AF, Conley T, Nürnbergger J, Baldrige LA, Clendenon JL, Dunn KW, Phillips CL. Three-dimensional imaging of human skin and mucosa by two-photon laser scanning microscopy. J Cutan Pathol 2002; 29: 453–458. © Blackwell Munksgaard 2002.

Janine C. Malone^{1,4},
Antoinette F. Hood¹,
Tameka Conley¹,
Jens Nürnbergger²,
Lee Ann Baldrige³,
Jeffrey L. Clendenon²,
Ken W. Dunn² and
Carrie L. Phillips^{2,3}

¹Department of Pathology and Laboratory Medicine, Division of Dermatopathology, ²Department of Medicine, Division of Nephrology, ³Department of Pathology and Laboratory Medicine, Indiana University School of Medicine, Indianapolis, IN, USA, and ⁴Department of Medicine, Division of Dermatology, University of Louisville School of Medicine, Louisville, KY, USA

Janine C. Malone MD, University of Louisville School of Medicine, Department of Medicine, Division of Dermatology, Department of Pathology and Laboratory Medicine,
Tel: +1-502 583 1749
Fax: +1-502 852 4720
E-mail: drj9@aol.com

Accepted September 7, 2001

Complex three-dimensional (3D) structures in human skin are difficult to analyze using conventional light microscopy and standard histologic techniques. Furthermore, the complicated morphology and arrangement of mucosal, dermal and epidermal components are lost when images are presented in standard two-dimensional (2D) displays. For instance, linear or branching structures such as blood vessels, adnexal structures and nerves appear as relatively simple geometric shapes when sectioned and imaged in various orientations along a 2D plane. In reality these structures comprise elaborate, 3D networks that interact to form the complex environment of the dermis. The extent of these 3D networks is such that the intricate *in situ* tissue architecture is not captured in thin (5–

6 µm) microtome sections. These networks are only apparent in thick sections that, when imaged by wide-field microscopy, appear blurred due to out-of-focus fluorescence. Thus thick samples must be imaged using instruments capable of providing thin optical sections of thick tissue samples, which can then be combined to provide 3D image volumes. Confocal laser scanning (single-photon) microscopy is typically used to collect such optical sections, but the effective depth of confocal imaging is limited by light scattering, and the collection of 3D volumes is hampered by the accrued photobleaching that occurs as the sample is repeatedly scanned by the laser. Scanning electron microscopy has the ability to image with sub-micrometer detail but this technology does not delin-

erate specific structural morphology using cell-specific markers such as fluorescently labeled antibodies or lectins.

The limitations of traditional microscopy have been addressed with two-photon microscopy. This method allows for deep, non-invasive, optical sectioning of fluorescently labeled biopsy specimens that are cut hundreds of micrometers in thickness. As with confocal imaging, two-photon microscopy can generate 3D images by overlaying sequential 2D optical slices. However, two-photon microscopy more efficiently collects scattered fluorescence, allows deeper penetration into tissues and reduces photobleaching. Image volumes may be rendered and displayed as detailed 2D or 3D images.

Data sets collected from two-photon microscopes are stored in computer files which typically contain 50–100 megabytes. 3D images are rendered from these large data sets using special volume visualization software that can analyze 3D pixels or 'voxels' (volume elements). We rendered our image volumes with Voxx.¹ Voxx is a novel volume rendering system that was designed to provide for rapid analysis of large, 3D data sets on low-cost computer systems. The software has been made freely available for non-commercial uses by the Indiana Center for Biological Microscopy, Indiana University School of Medicine, Indianapolis, IN. In summary, the tissue processing, imaging and analysis techniques herein described have considerable potential in examination of human skin biopsy specimens for diagnosis of diseases involving specific skin components that have previously been difficult to analyze.

Methods

Tissue preparation

The uses of archived, frozen human biopsy specimens were in accordance with guidelines established by the Institutional Review Board at Indiana University School of Medicine. Frozen tissue sections of skin cut at 60–150 μm were rinsed in tris buffered saline (TBS) for 10 min to remove OCT embedding material (Sakura Finetek USA, Inc., Torrance, CA). Frozen sections were fixed in 4% paraformaldehyde for 15 min, followed by a 30-min wash in TBS. Sections were incubated in blocking buffer containing 2% bovine serum albumin, 0.1% Triton X-100 and 1X phosphate-buffered saline (PBS) for 1 h at 25°C, then overnight at 4°C in rabbit antihuman PGP 9.5 antibody (1:3000 dilution, Biogenesis, Brentwood, NH). Secondary antibody (fluorescein-labeled goat-antirabbit, 1:200, Jackson ImmunoResearch Laboratories, West Grove, PA) was allowed to incubate overnight at 4°C. In some cases, rhodamine-labeled *Ulex europaeus* (1:200, Vector Laboratories, Burlingame, CA) was added concomitantly. All antibodies and lectins were

diluted in blocking buffer. After each incubation with antibody or lectin, sections were washed in two changes of TBS for 2 h. Sections were placed on glass bottom no. 1.5 culture dishes (MatTek Corp., Ashland, MA) with tissue held in place by a round glass coverslip (Fisher Scientific, Fair Lawn, NJ).

Image acquisition

Sections of fluorescently labeled skin were imaged on a Bio-Rad MRC 1024 confocal/2-photon system (Bio-Rad, Hercules, CA) fitted to a Nikon Eclipse inverted microscope with a 60X-water immersion, NA 1.2 objective (Nikon, Melville, NY). The objective was adjusted to match the coverslip thickness for each sample. Illumination was provided by a Spectra-Physics (Mountain View, CA) Tsunami Lite Titanium-Sapphire laser tuned to a wavelength of 820 nm. Data sets were collected as Z-series of 41–200 images with a spacing of 0.4 μm .

Image analysis

Real-time 3D image rendering was performed using Voxx software developed at the Indiana Center for Biological Microscopy, Indianapolis, IN (free download at <http://nephrology.iupui.edu/imaging/voxx/download>).¹ Voxx-generated movies accompany all figures and may be viewed at <http://www.nephrology.iupui.edu/malone>. All volume-rendered movies and the black and white panels in Figs. 1–3 were produced with the PC version of this software, which is written in C++ and uses OpenGL, GLUT and GLUI to control a NVIDIA GeForce2 graphics processor (NVIDIA Corp., Santa Clara, CA). Red-green anaglyphs (Figs. 1–3) and dual-color stereo pairs (Figs. 4 and 5) were prepared using Metamorph (Universal Imaging, West Chester, PA), and Photoshop (Adobe, Mountain View, CA).

Results

We have combined two-photon microscopy with 3D image analysis to evaluate structures within human skin and mucous membrane. Two-photon microscopy allowed us to visualize vascular, neural and adnexal structures within normal mucocutaneous tissue.

The lectin *Ulex europaeus* labels vascular structures and was found to react with follicular epithelium. Figure 1 demonstrates the complex, anastomosing vascular network seen in close proximity to a hair follicle using fluorescently labeled *Ulex europaeus* lectin. Animated rotations of this image (Movie 1) may be seen by accessing <http://www.nephrology.iupui.edu/malone>. Vessels appear to prominently surround the isthmus enforcing the critical role of this portion of the follicle in the hair cycle.

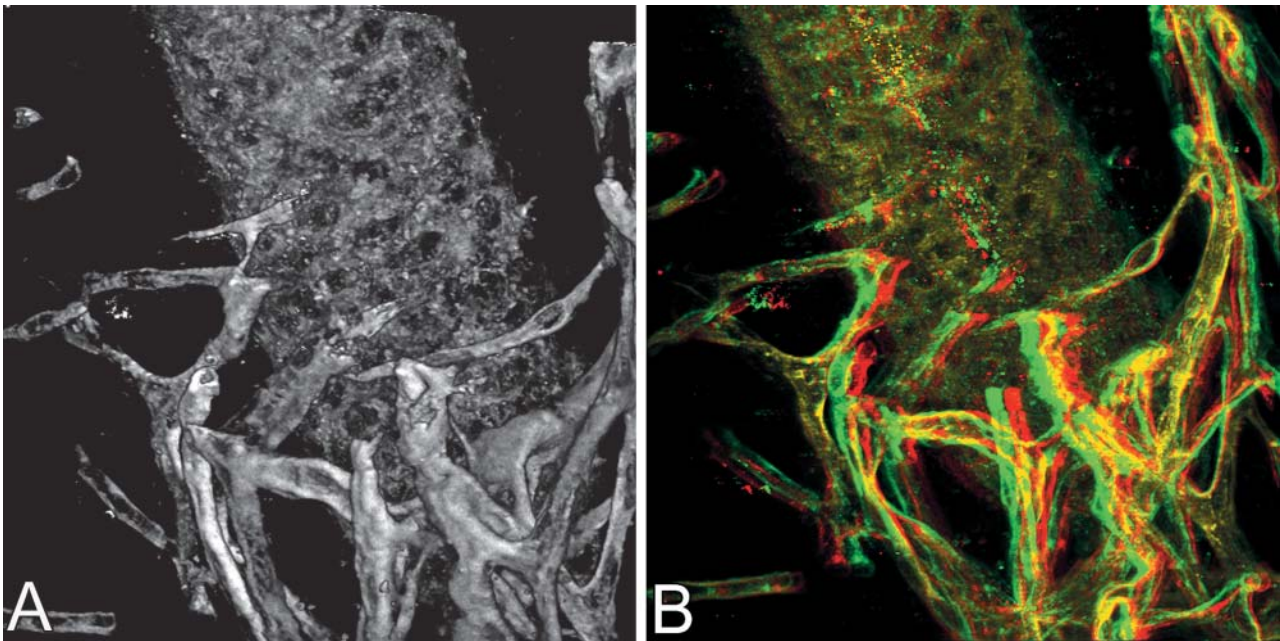


Fig. 1. Three-dimensional rendering of vascular supply of a hair follicle. Blood vessels surrounding a hair follicle in a thick section of human skin were labeled with *Ulex europaeus*-rhodamine. The volume was rendered with greater opacity in the Voxx-generated image (A) and more transparent in the red-green anaglyph (B, requires red-green glasses). Because the tissue section includes a representative portion of the entire follicular structure (isthmus), the follicle appears cropped in this image. There is endogenous fluorescence of melanin granules within the internal portions of the hair follicle. Movie 1 shows the Voxx-rendering and manipulation of the entire image volume (all movies can be viewed at <http://www.nephrology.iupui.edu/malone>), whereby one may better appreciate the cylindrical nature of the hair follicle as well as the 'concave' internal structure of the follicle when viewed from the posterior (inner root sheath) aspect. Pseudo-coloring has been applied to the Voxx-rendered movie. The image is a projection of 200 optical sections taken at 0.4 μm intervals and measures 80 (Z-axis) by 205 (X-axis) by 205 (Y-axis) μm .

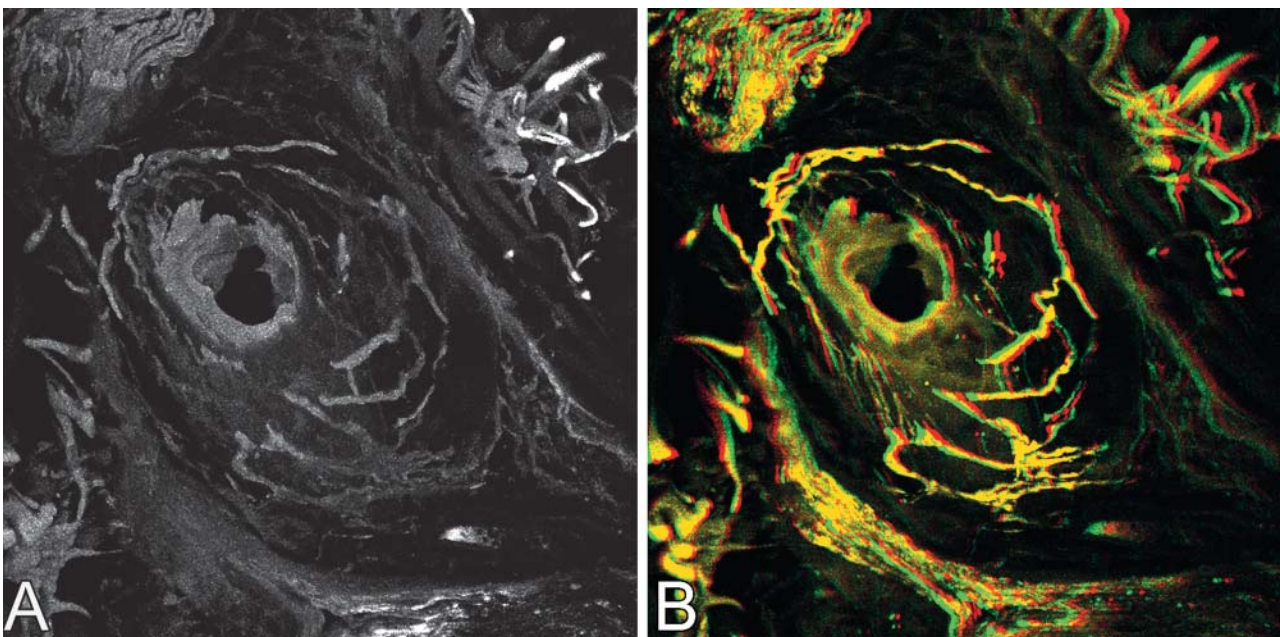


Fig. 2. Three-dimensional rendering of nerve supply to a hair follicle. Axonal terminals circumferentially located around the isthmus of a hair follicle are rendered in a thick section of human skin stained with anti-PGP 9.5-fluorescein. A) Voxx-rendered image. B) Red-green anaglyph (requires red-green glasses). The complex relationship of nerves and follicle are better displayed as a rotating image in Movie 2. The image is a projection of 41 optical sections and measures 16 \times 205 \times 205 μm .

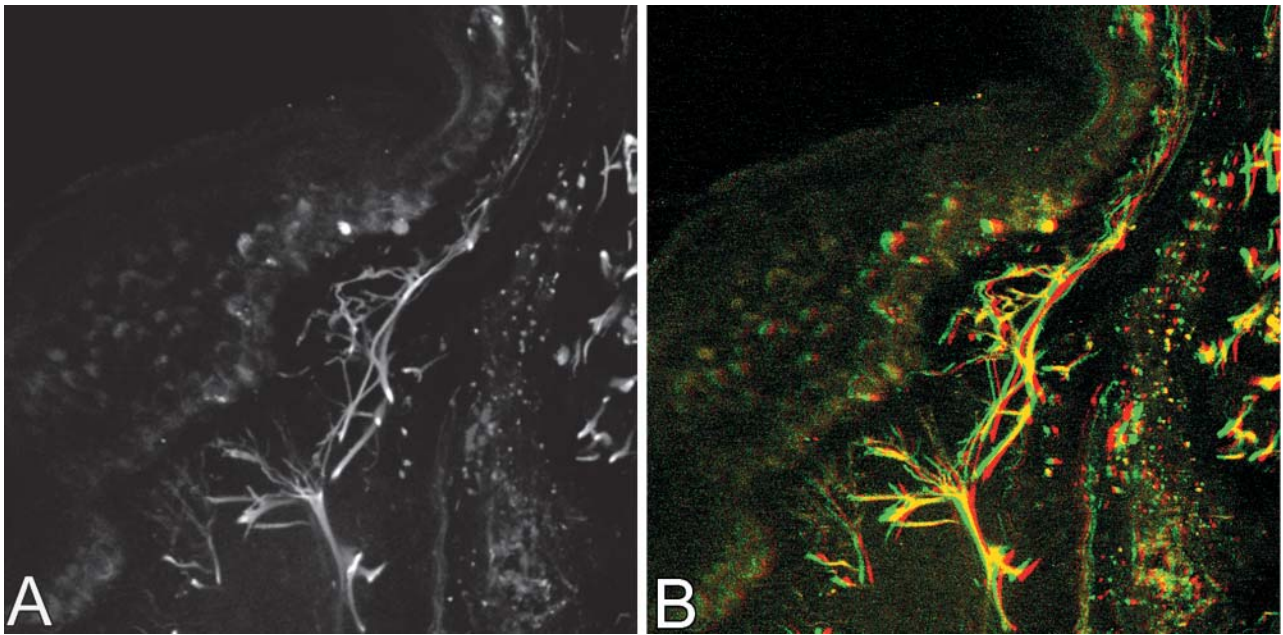


Fig 3. Three-dimensional rendering of subepidermal nerve plexus. Nerve terminals adjacent to the epidermis are labeled with anti-PGP 9.5-fluorescein. A) Vox-rendered image. B) Red-green anaglyph (requires red-green glasses). Large nerve bundles rise through the dermis to form a subepidermal neural plexus composed of dichotomously branching nerve fibers. The rotating image, seen in Movie 3, better illustrates the horizontal and vertically parallel arrangement of nerve fibers making up the plexus. The image is a projection of 76 optical sections and measures $30 \times 205 \times 205 \mu\text{m}$.

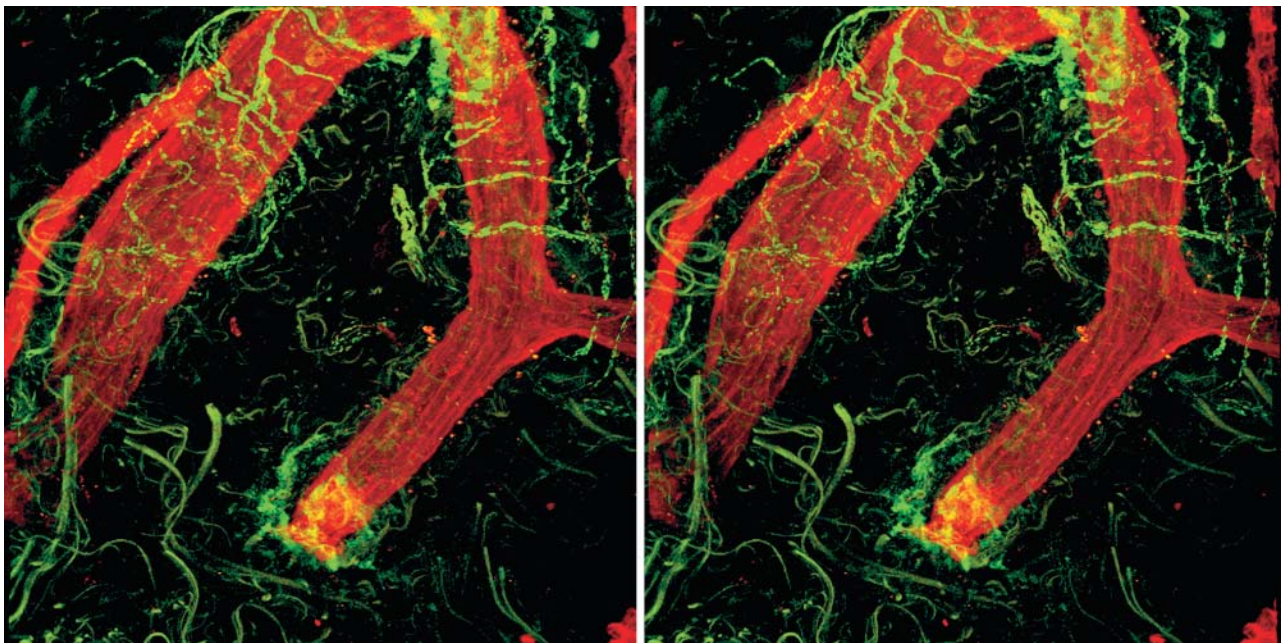


Fig 4. Dual-labeling of submucosal arterioles and nerves. Stereo pairs show deep submucosal blood vessels and nerves stained with *Ulex europaeus*-rhodamine (red) and anti-PGP 9.5-fluorescein (green), respectively. Arterioles are followed in parallel by nerve fibers that branch to encircle the vessel wall at variable points along its length. Rotations of the image volume (Movie 4) better demonstrate the convoluted morphology and complex interrelationship of these structures. The volume measures $44 \times 205 \times 205 \mu\text{m}$.

Dermal nerve bundles are best localized by antibodies to protein gene product 9.5 (PGP 9.5). Large nerve bundles in the subcutis and deeper portions of

the reticular dermis divide to innervate a variety of structures, including eccrine coils, hair follicles, and arterioles. Figure 2 and Movie 2 demonstrate inner-

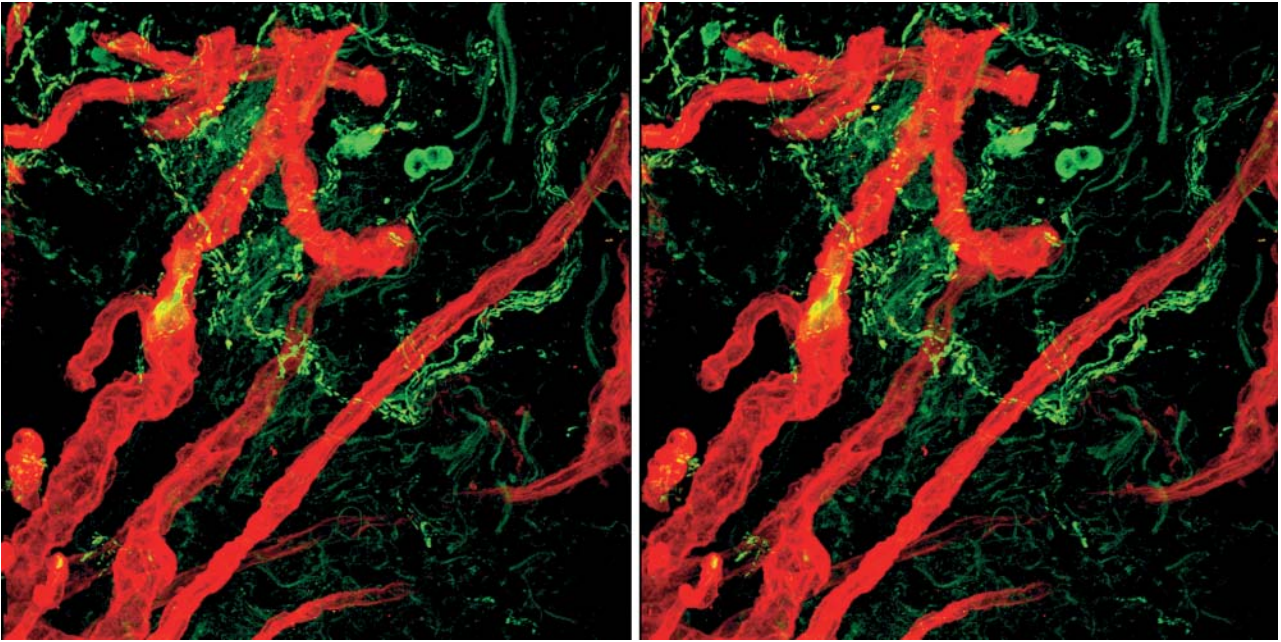


Fig. 5. Dual-labeling of submucosal capillaries and nerves. Stereo pairs show superficial submucosal blood vessels and nerves stained with *Ulex europaeus*-rhodamine (red) and anti-PGP 9.5-fluorescein (green), respectively. Capillaries have a more convoluted arrangement and are not so closely arrayed to nerve fibers. Rotations of the image volume (Movie 5) better demonstrate the convoluted morphology and complex interrelationship of these structures. The image volume measures $51 \times 205 \times 205 \mu\text{m}$.

vation of a hair follicle. Nerve axons appear to wrap around portions of the follicle and are most densely located in the region of the follicular isthmus. At the level of the upper reticular dermis, a plexus of nerve fibers arranged horizontally to the epidermis is visualized. This superficial plexus is composed of repeating units of these fibers arranged in parallel with each other. At variable points from within this plexus, small nerve fibers arise in a vertical fashion and branch dichotomously to enter the papillary dermis (Fig. 3 and Movie 3). Epidermal nerve fibers are not demonstrated with this technique, although nerve fibers entering the tips of dermal papillae sometimes appear intraepidermal in location when viewed adjacent to basal layers of epidermis.

Vascular structures in the dermis are commonly associated with nerve bundles and fibers. This finding is less constant in submucosal tissues. The association of two antigens in the same tissue is made possible by double staining with antibodies raised in different species or by combining an antibody and lectin, each labeled with different fluorescent markers (e.g. rhodamine or fluorescein). Structures are then visualized simultaneously using different filter sets. Figures 4 and 5 are dual-color, stereo pair images of submucosal nerves and blood vessels demonstrating the significant tortuosity of arterioles and capillaries (stained with *Ulex europaeus*-rhodamine) and associated nerve fibers (stained with anti-PGP 9.5 antibody-fluorescein). A stereo pair is constructed by projecting the image vol-

umes from two different angles. The stereoscopic images may be viewed with a stereo viewer. Alternatively, the two images may be fused into a 3D image either by crossing one's eyes or by focusing to an infinite distance until the two images converge. Although nerve fibers focally form a plexus surrounding the larger caliber vascular channels (Fig. 4), in many areas there is lack of significant contact between nerve fibers and capillaries (Fig. 5 – this is especially apparent in the movies). As expected, vascular structures are found in higher density in submucosal tissues compared with interadnexal areas of dermis.

Discussion

We have demonstrated the ability of two-photon microscopy to image various structural components of human skin and mucosa *in situ*. Not only does this method offer an entirely new perspective on mucocutaneous tissue structures compared with those obtained using conventional microscopy but, since the images are created by digitally 'sectioning' within intact tissues, there is potential that living tissues may be imaged *in vivo* and rendered in three dimensions using image processing software.² Compared with confocal microscopy, the method of two-photon microscopy used in the present study is capable of imaging structures in very thick tissue sections with improved contrast and resolution. In previous studies^{1,3} and in the present study, we have developed

and applied a user-friendly image-processing program capable of rapidly analyzing large data sets on inexpensive personal computers.

An understudied area in the field of dermatopathology involves morphologic variations in cutaneous blood vessels and nerves in normal and various pathologic states. These structures have a complex linear arrangement that is difficult to appreciate in standard 2D displays. Previously, analysis of these structures involved labor-intensive and subjective manual-counting methods that required multiple tissue sections.^{4,5} Again, because the images collected using two-photon microscopy are digitized, image analysis programs capable of objectively measuring parameters such as length, caliber and distance between branch points may be applied to detect subtle changes in nerve and vessel morphology in normal skin and skin affected by various pathologic conditions.

In the dermatopathology literature, there are few reports utilizing confocal microscopy in the study of cutaneous nerves. Reilly et al.⁶ studied the innervation patterns of epidermal nerves in various racial groups and found no apparent difference in innervation. Hordinsky & Ericson⁷ utilized confocal microscopy to describe follicular innervation differences in the normal and diseased states. Broadened to include a variety of literature sources, confocal microscopy has been utilized to study the innervation of human cutaneous melanocytes,⁸ the innervation and vasculature of human sweat glands,⁹ the structure of human Meissner corpuscles¹⁰ and Merkel complexes,¹¹ and cutaneous nerve reinnervation patterns.^{12,13} We are not aware of any studies that have utilized two-photon microscopy and 3D-rendering software to image these structures.

Two-photon microscopy and advanced digital imaging processing programs have revolutionized our ability to resolve structures within biologic tissues, offering an entirely new perspective in the fields of histology and histopathology. The methods described herein will be useful in further assessment of cutaneous pathology involving complex structures that have, until now, been difficult to analyze.

Acknowledgements

The authors wish to thank Christopher Moore and Heather Ward MT (ASCP) for their expert technical assistance with imaging and

image analysis. These studies were supported in part by INGEN, a grant from the Lilly Endowment to Indiana University School of Medicine.

References

1. Clendenon JL, Phillips CL, Sandoval RM, Fang S, Dunn KW. Voxo – a PC-based, near real-time volume rendering system for biological microscopy. *Am J Physiol Cell Physiol* 2002; 282: C213.
2. Masters BR, So PT, Gratton E. Multiphoton excitation fluorescence microscopy and spectroscopy of in vivo human skin. *Biophys J* 1997; 72: 2405.
3. Phillips CL, Arend LJ, Filson AJ et al. Three-dimensional imaging of embryonic mouse kidney by two-photon microscopy. *Am J Pathol* 2001; 158: 49.
4. Holland N, Stocks A, Hauer P et al. Intraepidermal nerve fiber density in patients with painful sensory neuropathy. *Neurology* 1997; 48: 708.
5. Stocks E, McArthur J, Griffen J, Mouton P. An unbiased method for estimation of total epidermal nerve fiber length. *J Neurocytol* 1996; 25: 637.
6. Reilly D, Ferdinando D, Johnston C, Shaw C, Buchanan K, Green M. The epidermal nerve fiber network: characterization of nerve fibers in human skin by confocal microscopy and assessment of racial variations. *Br J Dermatol* 1997; 137: 163.
7. Hordinsky M, Ericson M. Relationship between follicular nerve supply and alopecia. *Dermatol Clin* 1996; 14: 651.
8. Hara M, Toyoda M, Yaer M et al. Innervation of melanocytes in human skin. *J Exp Med* 1996; 184: 1385.
9. Kennedy W, Wendelschafer-Crabb G, Brelje T. Innervation and vasculature of human sweat glands: an immunohistochemistry-laser scanning confocal fluorescence microscopy study. *J Neurosci* 1994; 14: 6825.
10. Guinard D, Usson Y, Guillermet C, Saxod R. PS-100 and NF 70 double immunolabeling for human digital skin meissner corpuscle 3D imaging. *J Histochem Cytochem* 2000; 48: 295.
11. Guinard D, Usson Y, Guillermet C, Saxod R. Merkel complexes of human digital skin: three-dimensional imaging with confocal laser microscopy and double immunofluorescence. *J Compar Neurol* 1998; 398: 98.
12. Navarro X, Verdu E, Wendelschafer-Crabb G, Kennedy W. Immunohistochemical study of skin reinnervation by regenerative axons. *J Compar Neurol* 1997; 380: 164.
13. Simone D, Nolano M, Johnson T, Wendelschafer-Crabb G, Kennedy W. Intradermal injection of capsaicin in humans produces degeneration and subsequent reinnervation of epidermal nerve fibers: correlation with sensory function. *J Neurosci* 1998; 18: 8947.